

# Classification of Low Resolution Virtual Slides from Breast Tumor Sections: Comparison between Global and Local Analysis

Myriam Oger, Philippe Belhomme, Metin N. Gurcan, *Senior Member*

**Abstract—** In this paper, a comparison is made between a global and a local approach for computer-aided classification of virtual slides from breast tumor sections. The first approach classifies the images according to both color and texture information from the whole tissue, whereas the second one classifies them only on shape and texture from epithelial compartment. The originality of this study is that only low resolution virtual slides are used. As the cytological details are not visible at low resolution, the classification is only based on architectural aspect of each lesion. Experimental results on images from breast tumor sections show that some information is already present in low resolution virtual slides, allowing the classification in benign lesions versus malignant carcinomas.

## I. INTRODUCTION

BREAST cancer is the most common cancer among women in western countries. One in ten women is likely to develop breast cancer during her lifetime. In this context, the anatomical pathologist plays a key role in patient care. Indeed, after diagnosis, the surgery (mastectomy or not) and medical treatment (radiotherapy and/or chemotherapy) decisions depend on interpretation of macro and microscopic images of tissue sections. Observation of histological sections or cell preparations of tumors also allows the specialist to identify markers that can help to predict the survival chances of patients and their likelihood of recidivism. The role of specialist in pathology is central: he/she must provide a reliable and accurate diagnosis, including histological type of lesion, its grade and stage of expansion, and all of this within the shortest time possible. Because of wide-spread screening campaigns, the number of cases to be analyzed is constantly increasing, so is the workload of pathologists. In addition, early lesions discovered during screening are often poorly known and/or very small in size, which makes their histopathological

diagnosis very difficult. Every day pathologists perform an indispensable and challenging task, highly dependent on knowledge acquired through experience. However, inter- and intra-reader variability is well-documented and requires novel tools to help them.

In recent years, new scanning devices have appeared which can generate both low and high resolution virtual slides of the whole histological or cytological preparation. These systems produce digital images that can be browsed and shared with other experts, even at other institutions. These new means of acquiring images also enable capabilities to extract information from these images by processing and computerized analysis. It is therefore very important to assess how digital microscopy and automatic analysis tools of images can help specialists in carrying out their daily work. Some of the recent studies in this area are for example lung [1], prostate [2] cancers, follicular lymphoma [3] and neuroblastoma [4].

In this paper, we compare the use of global color and texture information as well as the use of local shape and texture information from hematoxylin-eosin-safron (HES)-stained images for an automated classification of breast lesions as benign or malignant carcinomas. It is important to be able to do this classification at low resolution because the algorithm can be run on a classical PC.

## II. FEATURE EXTRACTION AND CLASSIFICATION

### A. Database

The project is primarily dedicated to the study of histological sections of breast cancers. The section slides are digitized using the Nikon SuperCoolScan 8000 at a resolution of 4000 dot per inch. Each pixel represents an area of  $6.3 \times 6.3 \mu\text{m}^2$  (equivalent to a 2x magnification). A knowledge base was built with 209 virtual slides of the most frequently encountered histological subtypes of breast lesions. Those were collected in the pathology department of the François Baclesse cancer center, 57 images from benign tumors and 152 from malignant carcinomas, with an average disk size ranging from 60 to 70 Megabytes.

### B. Global Analysis

Initially, we focused on global analysis of slides by color and texture information without any segmentation except the separation between tissue and slide background.

1) *Color Features:* Concerning color, we used statistical

Manuscript received April 6, 2009. This work was supported in part by the Lower Normandy Region Council (France).

M. Oger is with the Quantitative Histo-Imagery team (GRECAN), François Baclesse Cancer Center, Ave du Général Harris, Caen 14076 Cedex 5, France (e-mail: [m.oger@baclesse.fr](mailto:m.oger@baclesse.fr)).

P. Belhomme is with the Quantitative Histo-Imagery team (GRECAN), François Baclesse Cancer Center, Ave du Général Harris, Caen 14076 Cedex 5, France (e-mail: [philippe.belhomme@unicaen.fr](mailto:philippe.belhomme@unicaen.fr)).

M. N. Gurcan is with the Department of Biomedical Informatics, The Ohio State University, 333 W. 10<sup>th</sup> Ave. Columbus, OH 43210, USA (e-mail: [metin.gurcan@osumc.edu](mailto:metin.gurcan@osumc.edu)).

features describing the shape of the color distribution which are mean, median, percentile, skewness and kurtosis, computed for each color component of RGB and/or YCh1Ch2 color spaces.

2) *Texture Features*: We have selected statistical Haralick features measured on grey level co-occurrence matrices [5] to analyze the texture.

Co-occurrence matrices are one of the most commonly used methods in texture description. Let  $\{I(x, y), 0 \leq x \leq N-1, 0 \leq y \leq M-1\}$  denote a grey-scale image, where  $G$  is the number of grey levels and  $N \times M$  is the image size, we can construct a  $G \times G$  grey-level co-occurrence matrix, named  $C_d$ , that gives the distribution of pair of pixels with a given relationship determined by the displacement vector  $d(d_r, d_c)$  as follows:

$$C_d(i, j) = \left| \left\{ (r, c) \mid I(r, c) = i \text{ and } I(r + d_r, c + d_c) = j \right\} \right|, \quad (1)$$

where  $(r, c), (r + d_r, c + d_c) \in N \times M$ .

The Fig. 1 shows four greylevel images and their corresponding co-occurrence matrices with  $d_r \leq 1$  and  $d_c \leq 1$ .

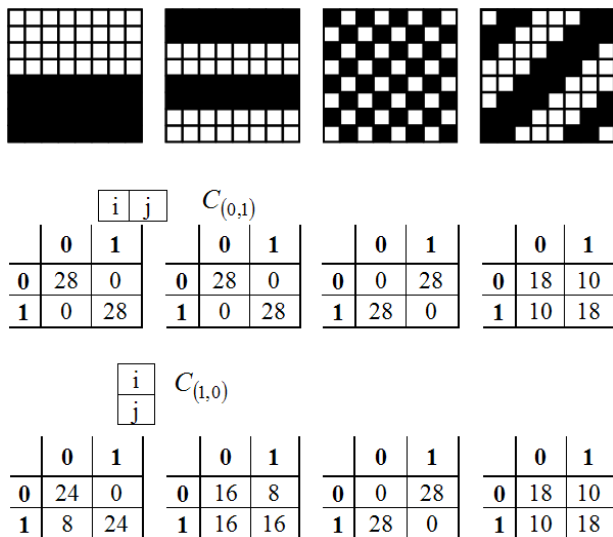


Figure 1: Co-occurrence matrices of four images with different textures

In order to construct the co-occurrence matrix, we first reduced the number of image grey levels from 256 to 16 by a linear transformation.

From the normalized and symmetrized matrix, we extracted five statistical features, defined by Haralick, namely energy, contrast, correlation, entropy and homogeneity.

Those color and texture features are the components of “signature” of each database image.

### C. Local Analysis

The differences between histological types of breast

lesions, benign tumor or malignant carcinoma, lie essentially in the epithelium abnormal aspect. To capture this information and so analyze those images locally, we had to segment each image into two compartments: stroma, whose color ranges between orange-pink and dark-pink, and epithelium, which is purple-blue.

1) *Segmentation*: At the segmentation step, we constructed a new feature space with both the  $a^*$  component from  $L^*a^*b^*$  color space, which represent an opposition between green and red, and the Ch2 component from the Carron color space (YCh1Ch2) [6], which is an opposition between green and blue and has a better contrast than  $b^*$  component (opposition between yellow and blue). The pixel classification was realized with an Expectation Maximization (EM) algorithm for 2D Gaussian mixture estimation. The number of clusters was defined by the number of modes of Ch2 grey-level distribution. As the Ch2 and the  $a^*$  grey-level distributions have several modes, they can be consider as Gaussian distribution mixtures. After the partition and a projection of each class barycenter on the Ch2 component, and than until there are at least two classes, the class with the higher projection value is grouped with those where the difference is less than 18 greylevels to constitute the epithelium class; the other classes are considerate as the different compartments of stroma (Fig. 2).

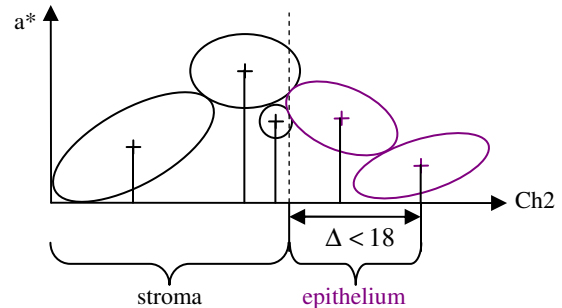


Figure 2: Example of a grouping of clusters in two classes

2) *Shape and Texture Features*: Shape features were measured on epithelial binary mask. We used the distribution of compactness, elongation or orientation and the number of nodes and branches of skeleton for each object corresponding to epithelial zones.

Texture features were computed on each greylevel component of RGB and YCh1Ch2 color spaces. Each component are masked with epithelial then stromal binary mask in order to capture the micro-texture features of those compartments by the extraction of Local Binary Pattern (LBP) features [7], which contain both structural and statistical information. In our previous work [8], we found these features to be useful for the classification of stromal regions in neuroblastoma. The LBP operator computes a binary pattern for each pixel by comparing the intensities of eight neighbor pixels to that of the center pixel. The Fig. 3 illustrates how the LBP operator computes the binary pattern

of a pixel on an example region of interest.

The LBP feature is calculated by:

$$LBP(p_c) = \sum_{i=0}^{N-1} 2^i \tau(p_i - p_c), \text{ where } \tau(x) = \begin{cases} 1 & x \geq 0 \\ 0 & x < 0 \end{cases}. \quad (2)$$

The histogram of these binary patterns is used to represent the texture of the image.

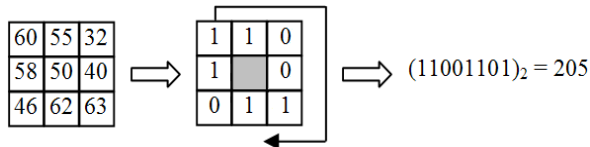


Figure 3: Result of the application of LBP operator on image sample presented on the left

Ojala *et al.* [7] extended the LBP operator and introduced a rotation-invariant uniform LBP features. Instead of using the conventional square neighborhood, they first constructed circular neighborhood for any given radius and number of samples around each pixel using bilinear interpolation. They defined the uniform LBP as circular patterns that contain at most two bitwise transitions from 0 to 1 or vice versa in its circular string. These patterns are referred to as bright spot, flat area, dark spot and edges of varying positive and negative curvatures. The authors experimentally showed that the uniform patterns account for almost 90% of all patterns in texture images with the configuration of one pixel radius and eight samples on the circular pattern.

3) *Dimensionality Reduction* [9]: As we known that the number of features can degrade the overall classification performance, we applied a feature selection step to improve the performance of classification by local features. In our application, feature selection is the process of selecting the best subset of features to maximize the discrimination between the two classes, benign lesion and malignant carcinoma.

We applied the feature selection step in an off-line manner only at the training step to remove the redundancy and determine the best subset of features. Among several feature selection algorithms, we employed Sequential Floating Forward Selection (SFFS) method [10], [11], which has been shown to be superior to other existing sequential procedures. Our optimization criterion for the feature selection was the classification accuracy over the training data. We selected the subset of features that maximized the leave-one-out cross-validation.

#### D. Classification

For the classification, we used the K-nearest neighbor (KNN) classifier. KNN classifier provides a robust performance since it does not require the estimation of the underlying distribution of the class samples, instead it estimates the local density. Therefore, it yields highly adaptive behavior on different datasets. Traditionally, the

KNN classifier assigns patterns to the majority class among the k-nearest neighbor in the training samples. In our implementation, we used  $k = 1, 3, 5$  or  $9$  as the number of neighbors.

The classification is made by a comparison between each element of the image signature from the database using the Mahalanobis or Kullback-Leibler distances.

The Mahalanobis distance uses the covariance matrix  $C$  of studied features. The distance is obtained by the following matricial computing:

$$M = \sqrt{(x_1 - x_2)^T C^{-1} (x_1 - x_2)}, \quad (3)$$

where  $x_1$  and  $x_2$  are feature values for images 1 and 2.

The Kullback-Leibler distance is calculated as follows:

$$KL = \sum_{i=1}^n (KL(x_1(i), x_2(i)) + KL(x_2(i), x_1(i))) \quad (4)$$

where  $n$  is the total number of features and  $KL(x, y) = x \log(x/y)$  is the Kullback-Leibler divergence.

This distance reduces the amplitude variations of values in a same set with the logarithm.

### III. EXPERIMENTAL RESULTS

If we only consider the distinction between benign and malignant carcinoma with a global analysis (Table I), a 69% accuracy can be achieved using RGB color features or 75% using YCh1Ch2 color features. But, in both cases, the benign class accuracy is less than 60%. The additional of texture features do not improve the results. This can be due to the fact that breast lesions are mostly heterogeneous.

TABLE I  
RESULTS OBTAINED WITH GLOBAL ANALYSIS ON 209 IMAGES WHEN CONSIDERING ONLY THE DISTINCTION BETWEEN BENIGN AND MALIGNANT CARCINOMA AND THE NEAREST NEIGHBOR

Percentage of good classified images (1st response)	Benign	Malignant carcinoma	Global
Color 24 RGB features (M)	59.65 %	73.03 %	69.38 %
Color 24 YCh1Ch2 features (KL)	52.63 %	84.21 %	75.06 %
Texture 5 Haralick features (M)	47.37 %	76.32 %	68.42 %
Color + Texture 24 RGB + 5 Haralick features (M)	42.11 %	78.29 %	68.42 %
Random Ranking*	28.07 %	67.76 %	56.94 %

KL: Kullback-Leibler Distance, M: Mahalanobis Distance

\*As there are about three times more malignant carcinoma cases than benign cases, the probability to take a malignant carcinoma case is really higher than to take a benign case. So, with the random ranking, the probability to take a benign case when you have already a benign virtual slide is very low.

A result of the pixel classification method, which allows the separation between stroma and epithelium, is presented in Fig. 4.

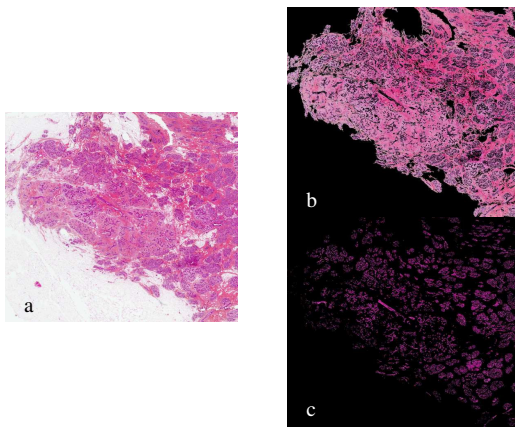


Figure 4: Result of the segmentation by EM pixel classification with, a) the original image, b) the stroma, and, c) the epithelium

Stromal and epithelial compartments being segmented, several features of texture and shape have been computed on the epithelium only or on both the epithelium and the stroma taken individually.

The computed features were selected using the SFFS method, after a dimensional reduction by PCA then LDA. After achieving the classification by k-means, the Leave-one-out cross validation has been used to evaluate the relevance of the selected feature subset.

A shape feature, the standard deviation of the compactness, and a texture feature, the LBP mean of the epithelium on the red component, have been selected as the more relevant features. The benign versus malignant carcinoma classification performance, obtained with only those two parameters, are compared to the results of the previous global study in the Table II.

TABLE II  
RESULTS OBTAINED WITH GLOBAL OR LOCAL ANALYSIS ON 209 IMAGES

Percentage of good classified images (1st response)		Benign	Malignant carcinoma	Global
Global Analysis	24 Color features	59.65 %	73.03 %	69,38 %
Local Analysis	1 Shape + 1 Texture features	<b>77.19 %</b>	<b>69.74 %</b>	<b>71.77 %</b>
Random Ranking		28.07 %	67.76 %	56.94 %

The classification performance is above 70% when we consider the benign and malignant carcinoma classes individually as well as together. The mean performance is equivalent to that obtained with the global analysis and the rate of correct classification of benign tumors is more than 2.7 times higher than for a random ranking.

#### IV. CONCLUSION

The classification of low-resolution images taken as a whole is possible by a global analysis and computing of color features, but this strategy is crude and can therefore only lead to a pre-classification of images. The segmentation

and the texture and shape features are also very promising for discrimination between benign and malignant lesions.

So, even at low resolution, we can already extract relevant information from histological section virtual slides, but it is not sufficient to achieve a complete separation between malignant and benign tumors.

To progress in this direction, it is desirable to explore the pathologist with his working method: what objective is used for what diagnosis? What magnification is required to resolve the differential diagnosis...

In our future work, we will complete the local analysis by expanding the feature set as well as combine global and local information in order to improve the overall classification results.

#### ACKNOWLEDGMENT

The authors want to thank Olcay Sertel for his help for the segmentation and local texture computation algorithms.

They also thank Dr. Jean-Jacques Michels, from the Pathology lab of François Baclesse Cancer Center, who has provided the histological sections of breast lesions and their corresponding diagnosis.

#### REFERENCES

- [1] K. Kayser, D. Radziszowski, P. Bzdyl, R. Sommer and G. Kayser, "Towards an automated virtual slide screening: theoretical considerations and practical experiences of automated tissue-based virtual diagnosis to be implemented in the Internet," *Diagnostic Pathology*, 2006, pp. 1-10.
- [2] S. Doyle, A. Madabhushi, M. Feldman and J. Tomaszewski, "A boosting cascade for automated detection of prostate cancer from digitized histology," *Med Image Comput*, 2006, vol. 9, no. 2, pp. 504-511.
- [3] O. Sertel, J. Kong, U. V. Catalyurek, G. Lozanski, J. Saltz and M. N. Gurcan, "Histopathological image analysis using model-based intermediate representations and colour texture: Follicular lymphoma grading," *The Journal of Signal Processing Systems*, May, 2008
- [4] O. Sertel, J. Kong, H. Shimada, U. V. Catalyurek, J. H. Saltz and M. N. Gurcan, "Computer-aided prognosis of neuroblastoma on whole-slide images: Classification of stromal development," *Pattern Recognition*, vol. 42, no. 6, 2009, pp. 1093-1103
- [5] R. Haralick, K. Shanmugan and I. Dinstein, "Textural features for image classification," *IEEE Transaction on Systems, Man and Cybernetics*, vol. 3, no. 6, 1973.
- [6] T. Carron, "Segmentation d'images couleur dans la base Teinte-Luminance-Saturation: approche numérique et symbolique," *PhD thesis*, University of Savoie, France, 1995.
- [7] T. Ojala, M. Pietikainen and T. Maenpaa, "Multiresolution gray-scale and rotation invariant texture classification with local binary patterns," *IEEE Transactions on PAMI*, vol. 24, no. 7, 2002, pp. 971-987.
- [8] O. Sertel, H. Shimada, U. V. Catalyurek, J.H. Saltz and M. N. Gurcan, "Computer-aided prognosis of neuroblastoma: classification of stromal development on whole-slide images," *Proc. of SPIE Medical Imaging*, vol. 6915, March 2008.
- [9] R. O. Duda, P. E. Hart, and D. G. Stork, *Pattern Classification*, 2001 Wiley.
- [10] P.A. Devijver and J. Kittler, "Pattern recognition: A statistical approach," Prentice-Hall, London, 1982.
- [11] P. Pudil, J. Novovicova and J. Kittler, "Floating search methods in feature selection," *Pattern Recognition Letters*, vol. 15, 1994, pp. 1119-1125.